Neural Networks in Real-Time Applications

Branko Souček

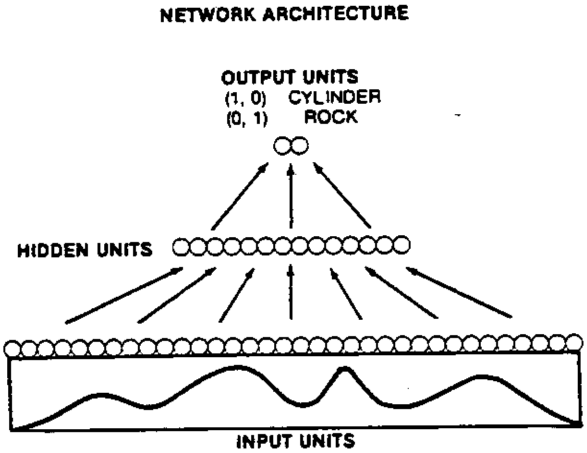

FIGURE 1. Schematic diagram of the network. The bottom layer has 60 processing units with their states "clamped" to the amplitude of the pre-processed sonar signal, shown in analog form below the units. The two output units at the top represent the two sonar targets to be identified. The layer of hidden units between the input and output layers allows the network to extract high-order signal features. The connections between the layers of units are represented by arrows.

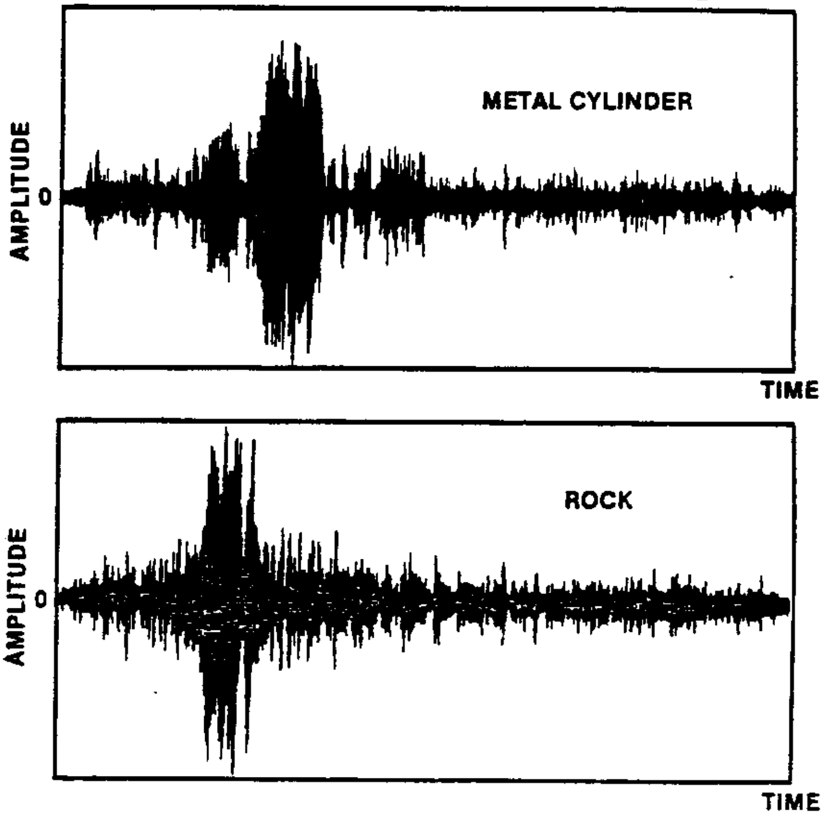

FIGURE 2. Amplitude displays of a typical return from the cylinder and the rock as a function of time.

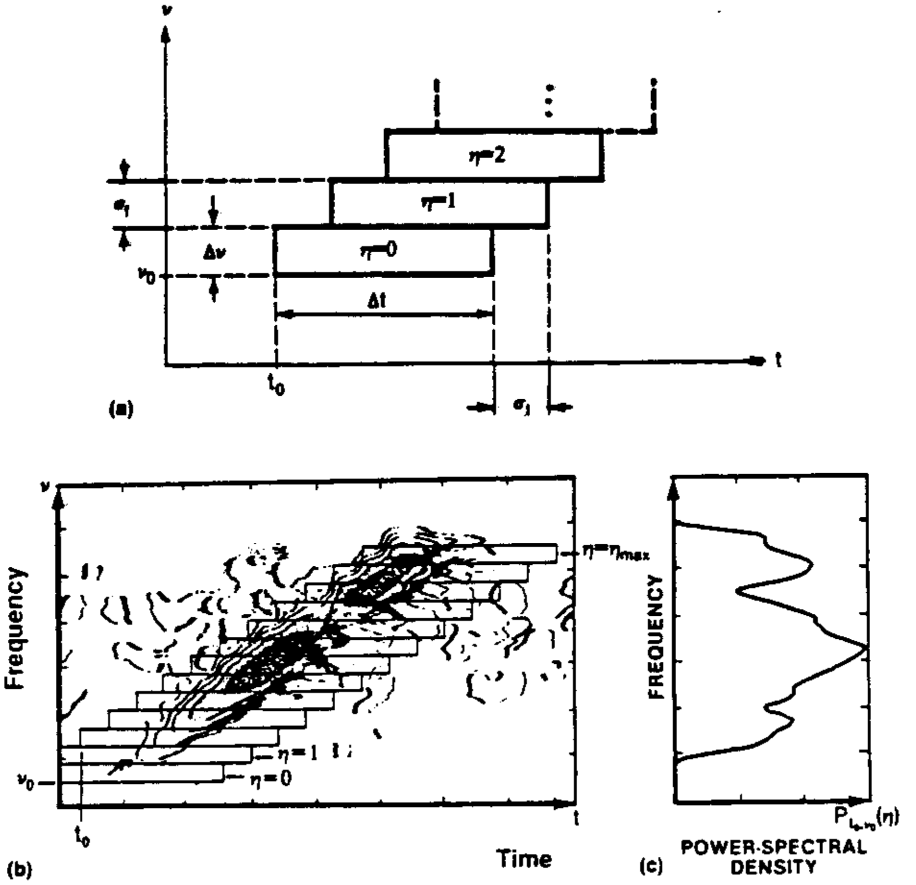

FIGURE 3. The preprocessing of the sonar signal produces a sampled spectral envelope normalized to vary from 0.0 to 1.0 input to the network. (a) The set of sampling apertures offset temporally to correspond to the slope of the FM chirp, (b) sampling apertures superimposed over the 2D display of the short-term Fourier transform, (c) the spectral envelope obtained by integrating over each sampling aperture.

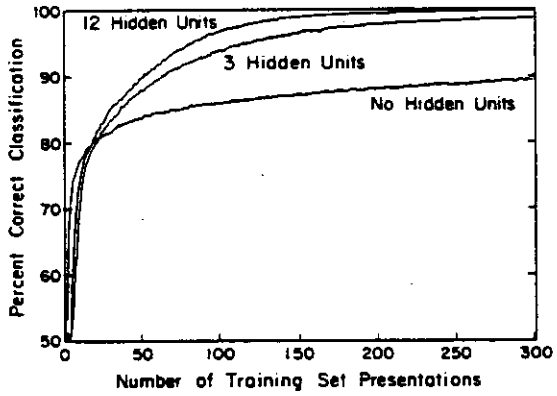

FIGURE 4. Network learning curves for the aspect-angle independent series of experiments using randomly chosen training sets. Each curve represents an average of 130 learning trials for a network with the specified number of hidden units.

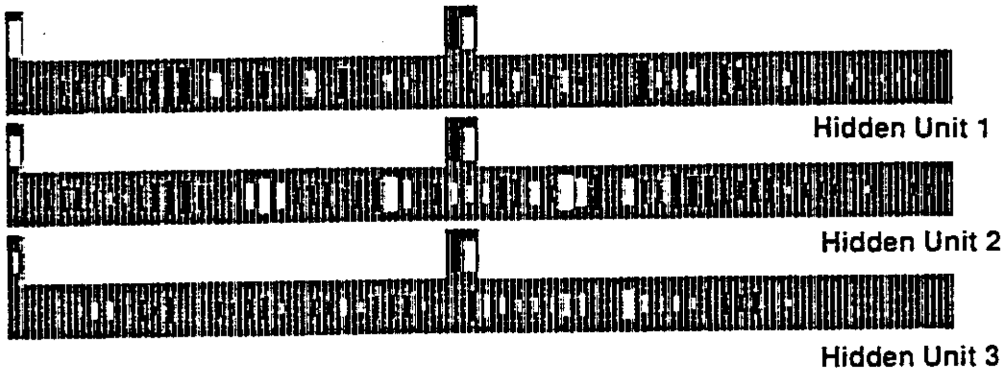

FIGURE 5. The weight pattern for a trained network with three hidden units. See text for explanation.

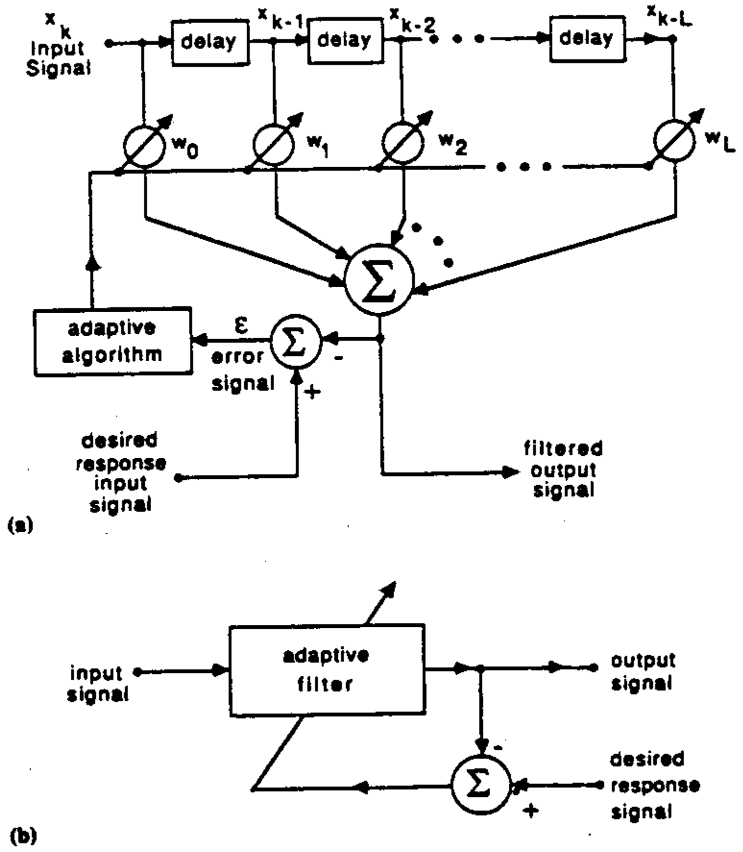

Figure 6. Adaptive digital filter: (a) details of a tapped-delay-line digital filter; (b) symbolic representation of an adaptive filter.

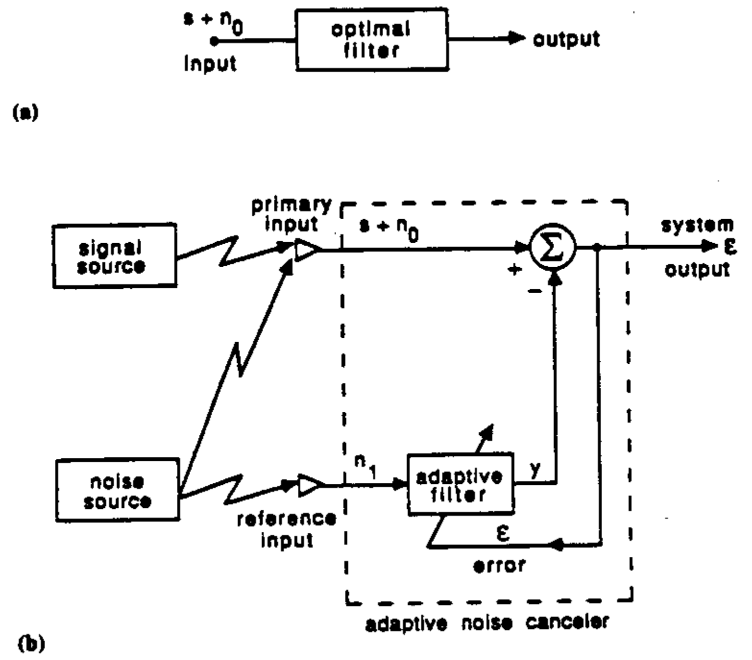

Figure 7. Separation of signal and noise: (a) classical approach; (b) adaptive noise-canceling approach.

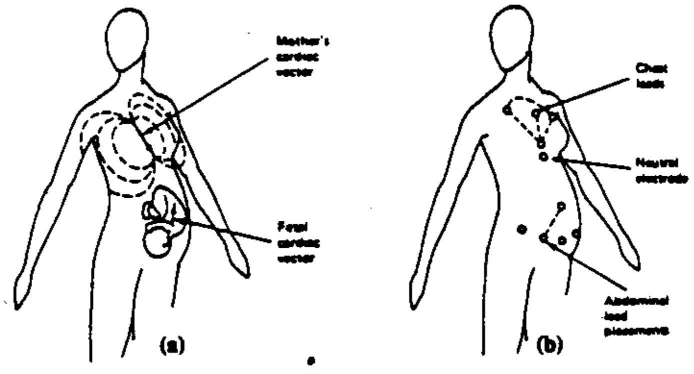

Figure 8. Canceling maternal heartbeat in fetal electrocardiography: (a) cardiac electric field vectors of mother and fetus; (b) placement of leads.

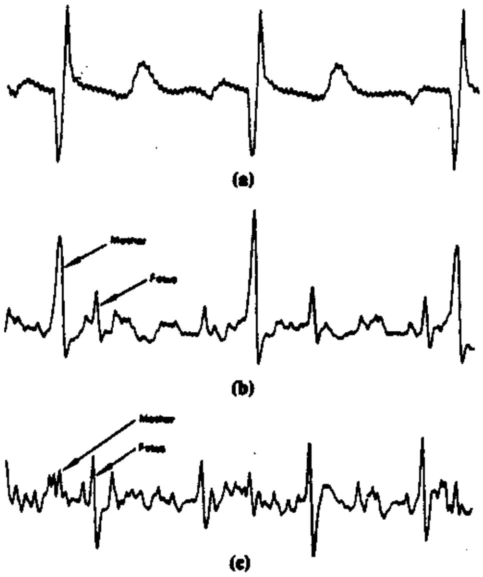

Figure 9. Result of fetal ECG experiment (bandwidth, 3-35 Hz; sampling rate, 256 Hz): (a) reference input (chest lead); (b) primary input (abdominal lead); (c) noise canceler output.

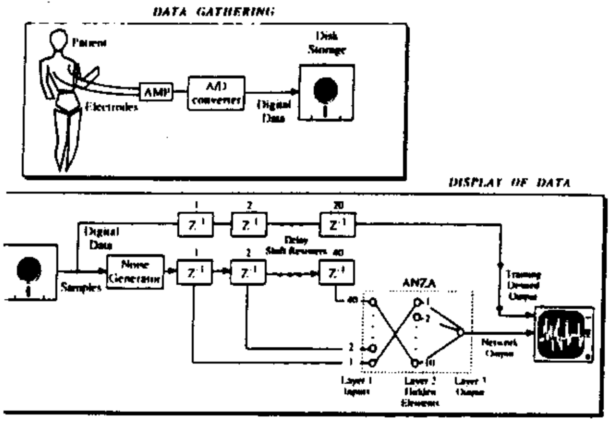

Fig. 10

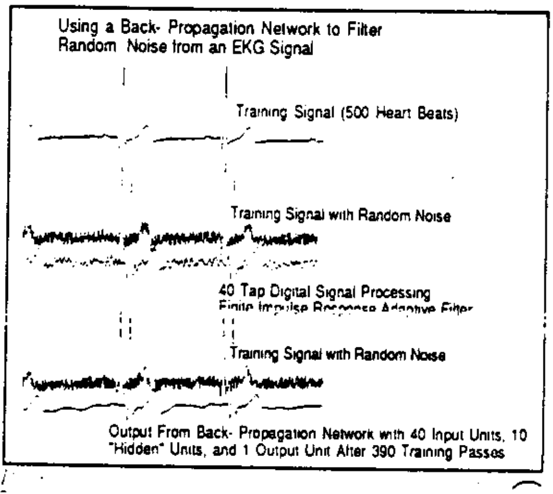

Fig 11

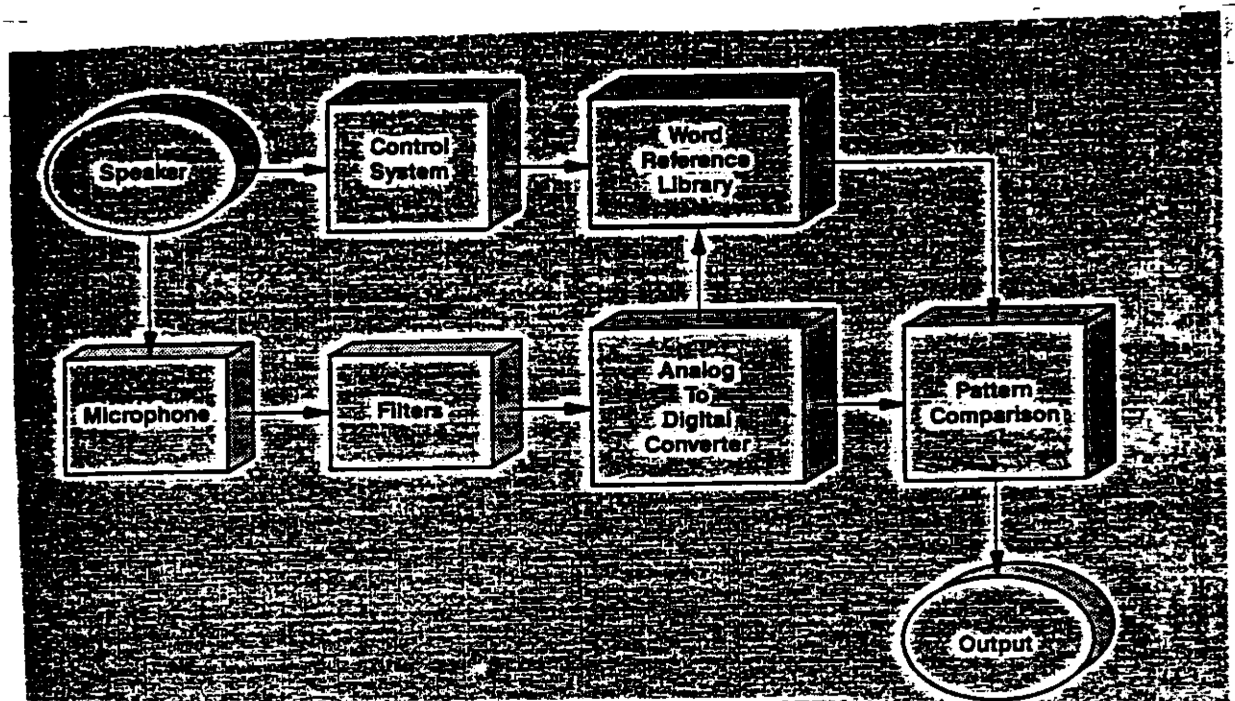

TYPICAL VOICE RECOGNITION SYSTEM
Figure 12

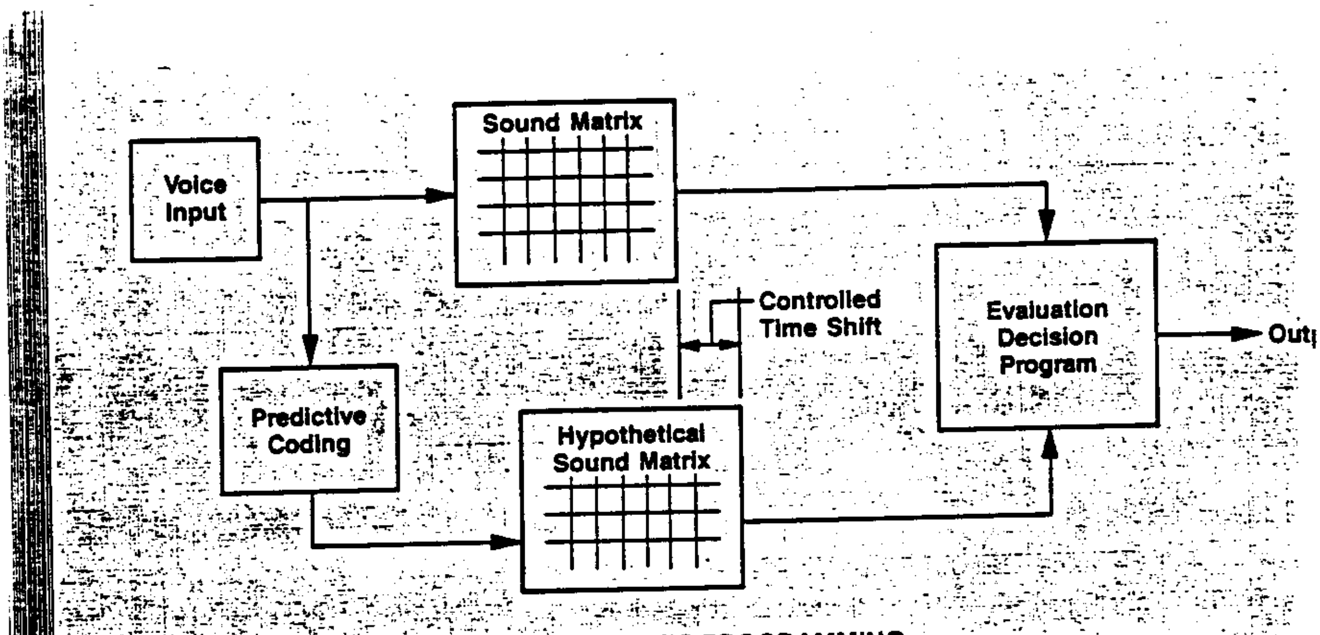

DYNAMIC PROGRAMMING
Figure 13

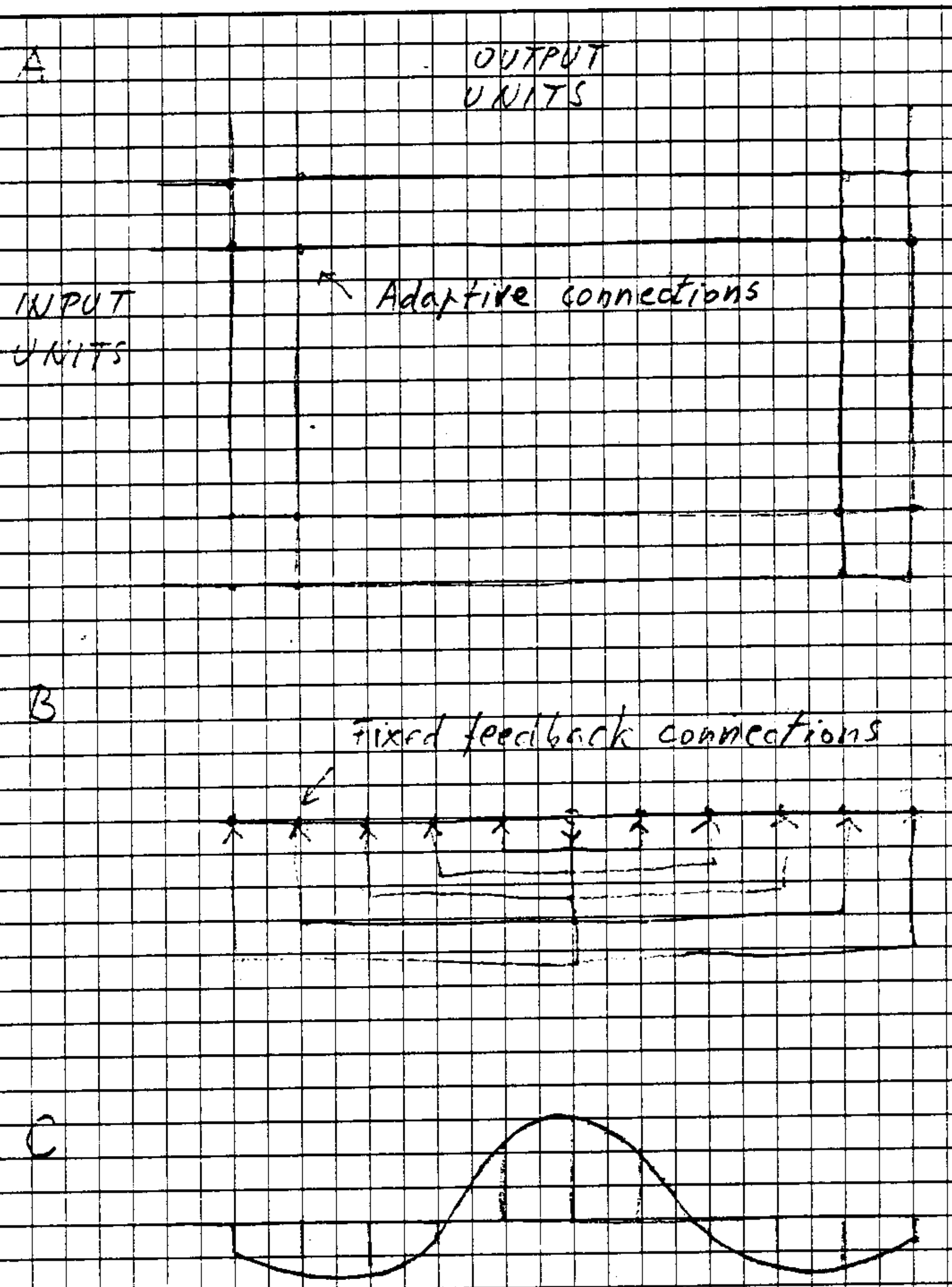

Kohonen Phonetic Typewriter

FIG. 14

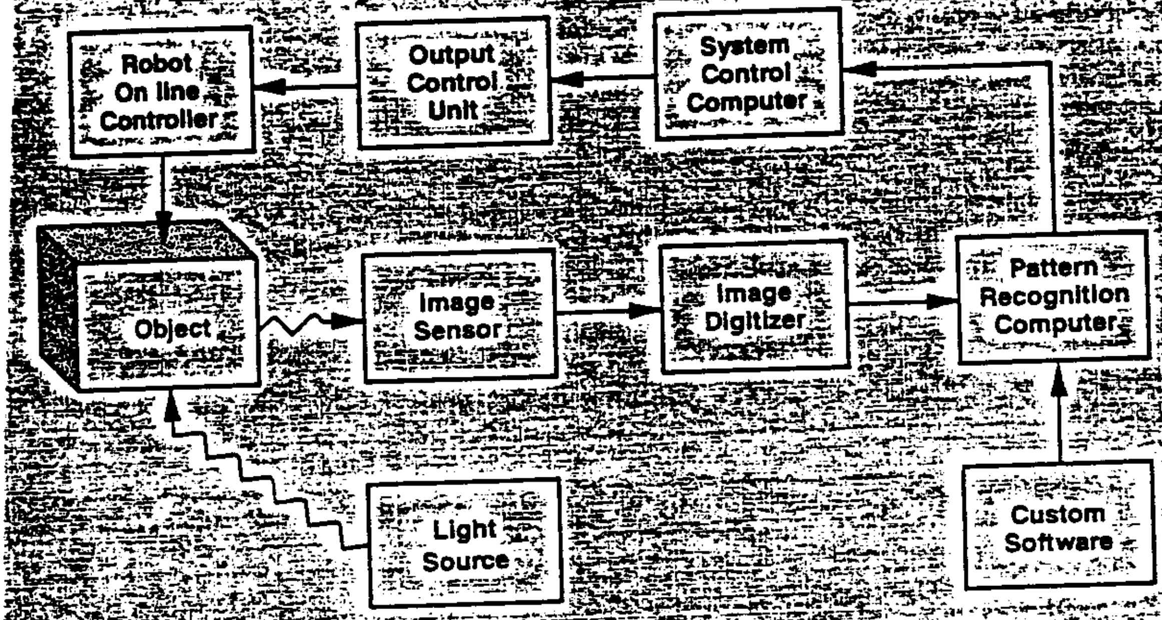

TYPICAL MACHINE-VISION SYSTEM
Figure 15

PROPOSED ANS EXPERIMENTAL DESIGN

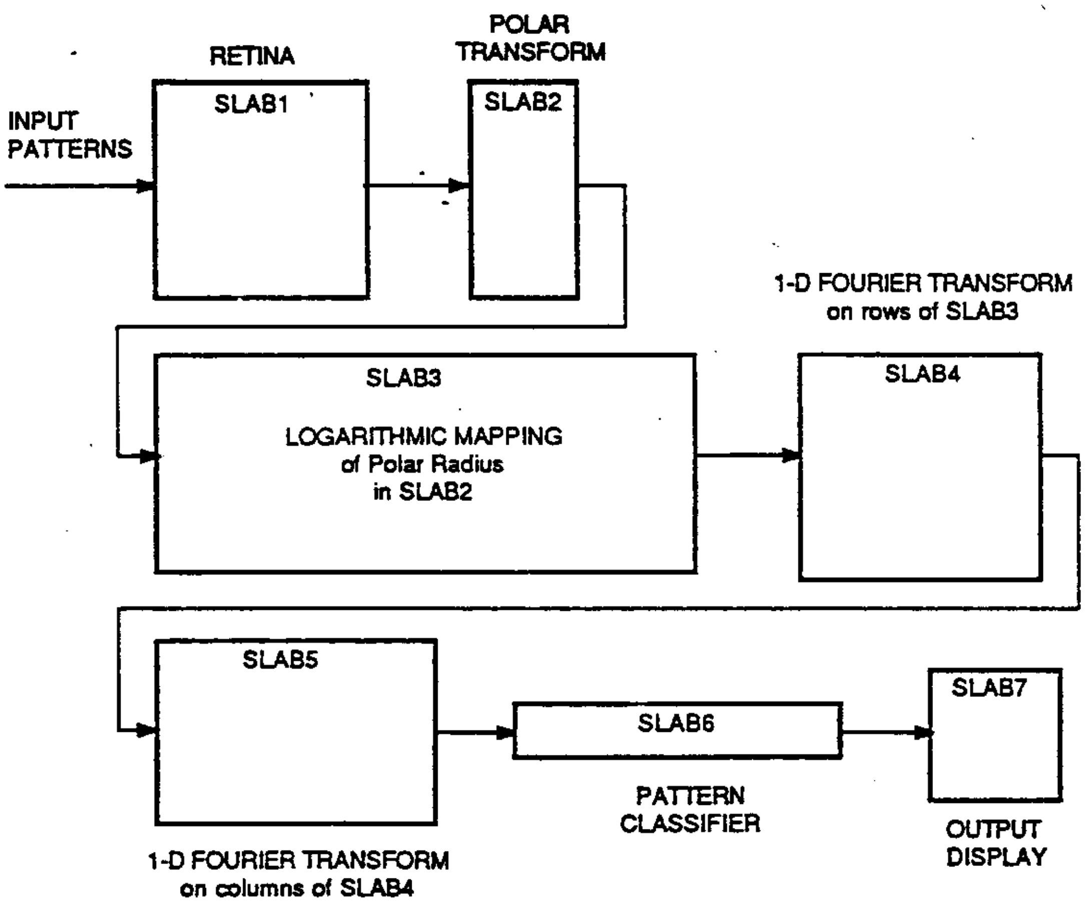
INPUT PATTERNS
RETINA
SLAB1
POLAR TRANSFORM
SLAB2
1-D FOURIER TRANSFORM on rows of SLAB3
SLAB3
LOGARITHMIC MAPPING of Polar Radius in SLAB2
SLAB4
SLAB5
SLAB6
SLAB7
PATTERN CLASSIFIER
OUTPUT DISPLAY
1-D FOURIER TRANSFORM on columns of SLAB4

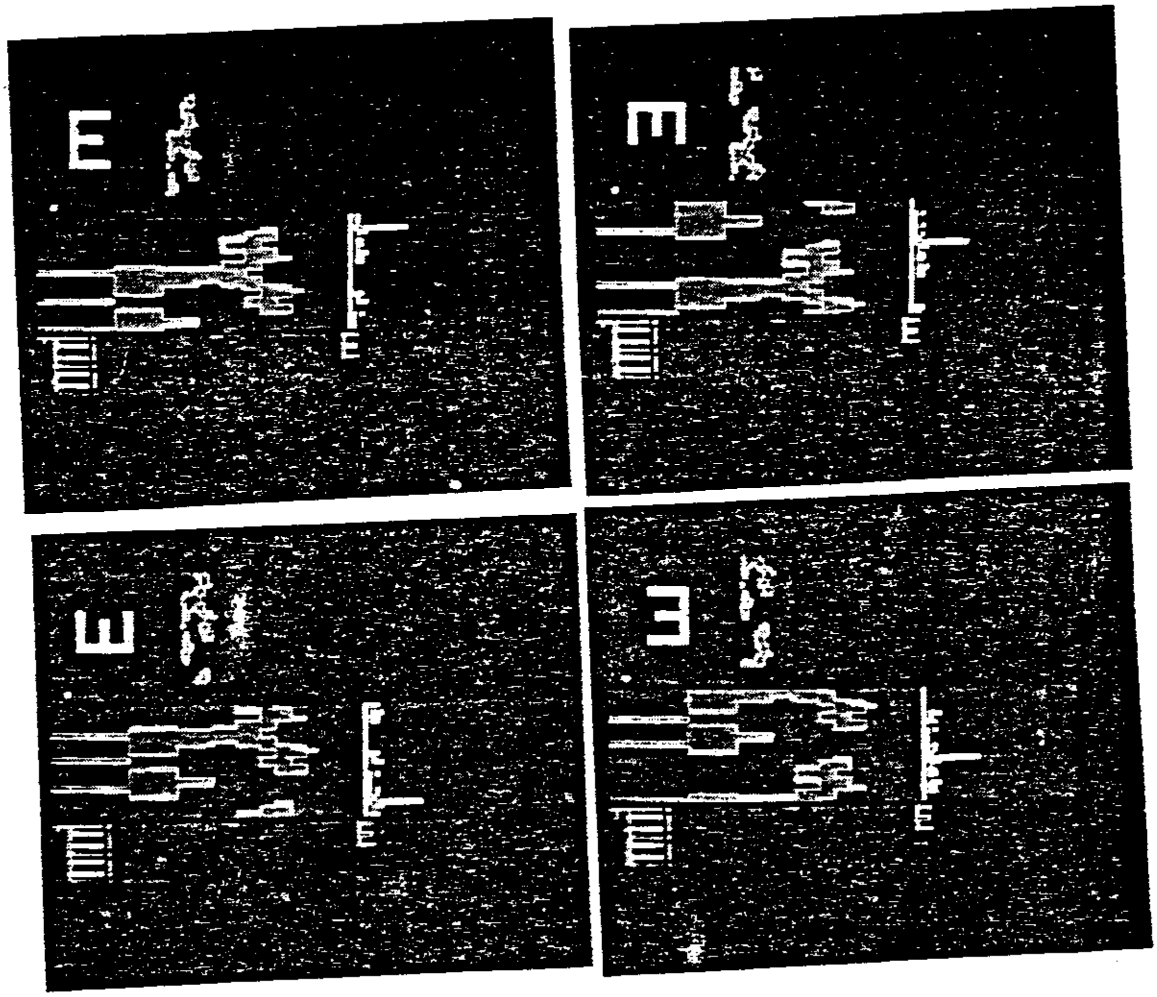

Figure 17 Rotation and Scale Invariant Classification of E

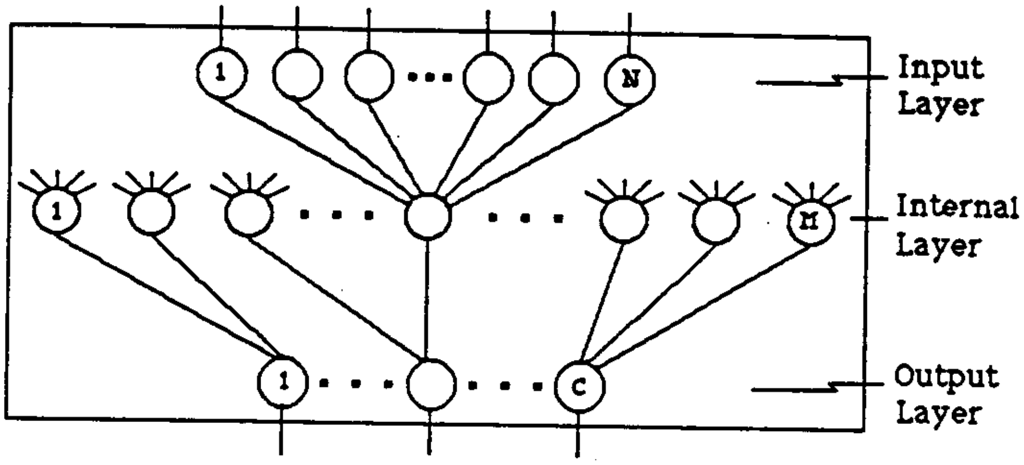

RCE Network
Figure 19

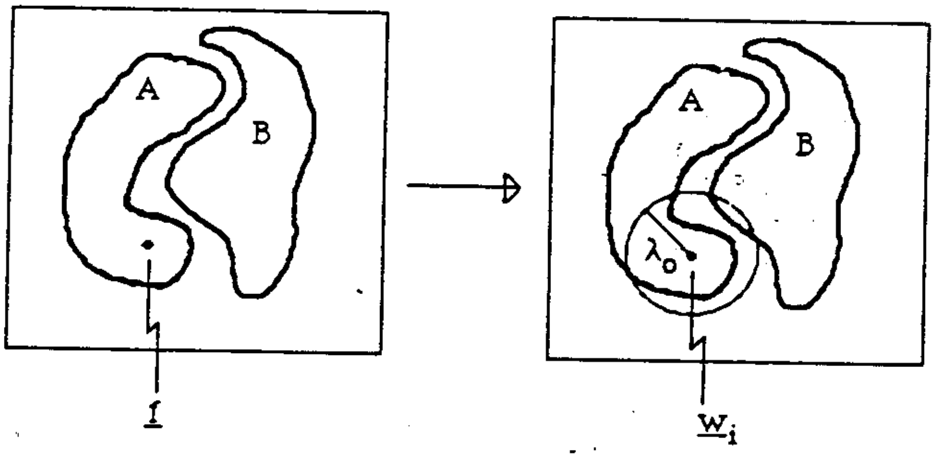

Feature space representation of cell commitment in internal layer.
Figure 20

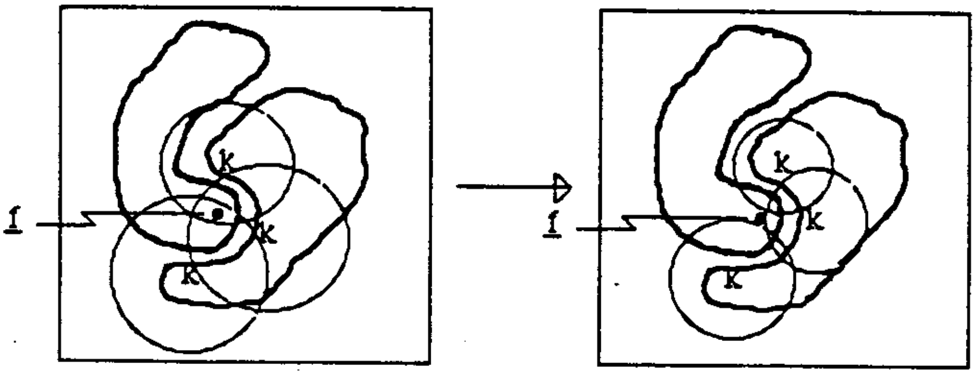

Threshold reduction for active internal layer cells associated with k^{th} output cell. After modification, $\underline{f}$ is no longer covered by any internal cell disc for k^{th} output cell.
Figure 21

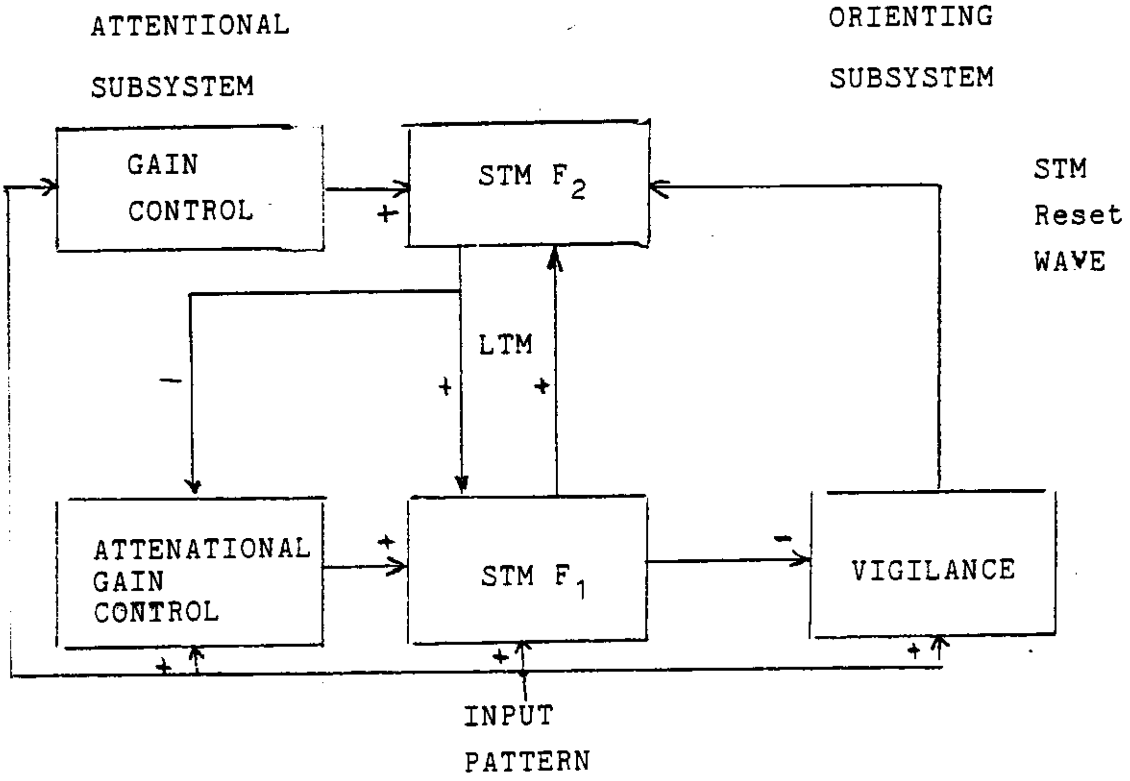

ART Network

Figure .22

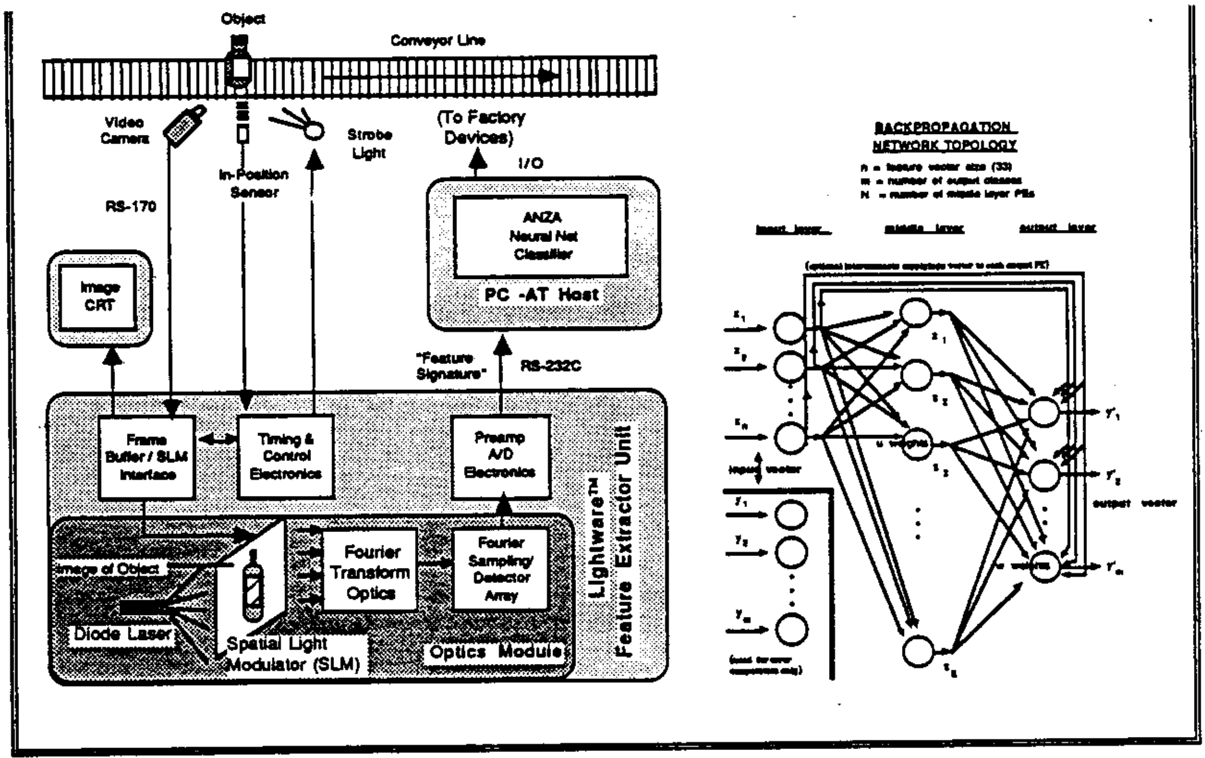
Object
Conveyor Line
Video Camera
Strobe Light
In-Position Sensor
(To Factory Devices)
I/O
RS-170
ANZA Neural Net Classifier
PC -AT Host
Image CRT
"Feature Signature"
RS-232C
Frame Buffer / SLM Interface
Timing & Control Electronics
Preamp A/D Electronics
Lightware™ Feature Extractor Unit
Image of Object
Fourier Transform Optics
Fourier Sampling/ Detector Array
Diode Laser
Spatial Light Modulator (SLM)
Optics Module
BACKPROPAGATION NETWORK TOPOLOGY
n = feature vector size (33)
m = number of output classes
N = number of middle layer PEs
input layer
middle layer
output layer
input vector
output vector

Fig. 15

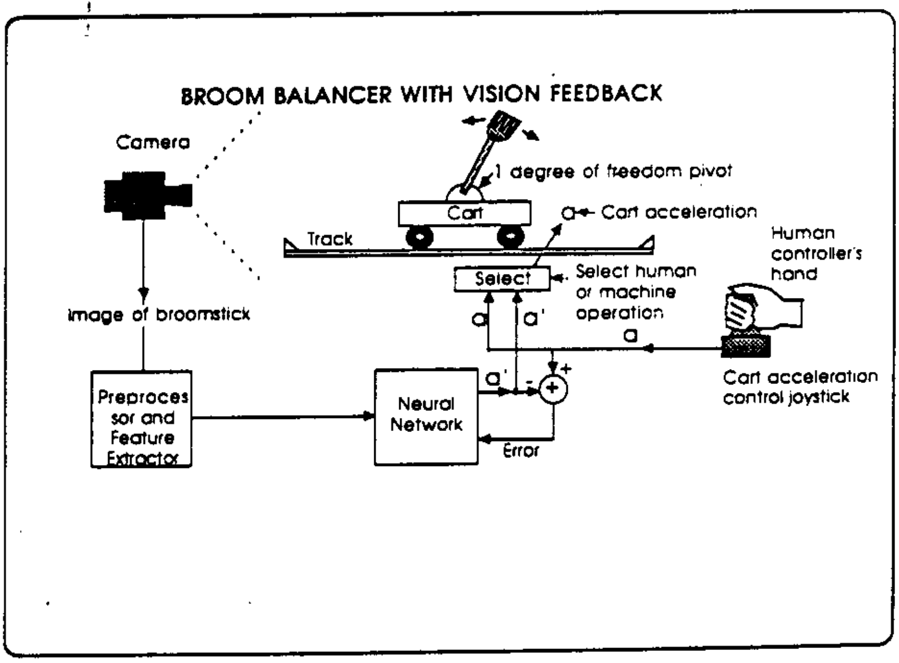
BROOM BALANCER WITH VISION FEEDBACK
Camera
1 degree of freedom pivot
Cart
a Cart acceleration
Track
Human controller's hand
Select
Select human or machine operation
Image of broomstick
a
a'
a
a'
-
+
Preprocessor and Feature Extractor
Neural Network
Error
Cart acceleration control joystick

Figure 27

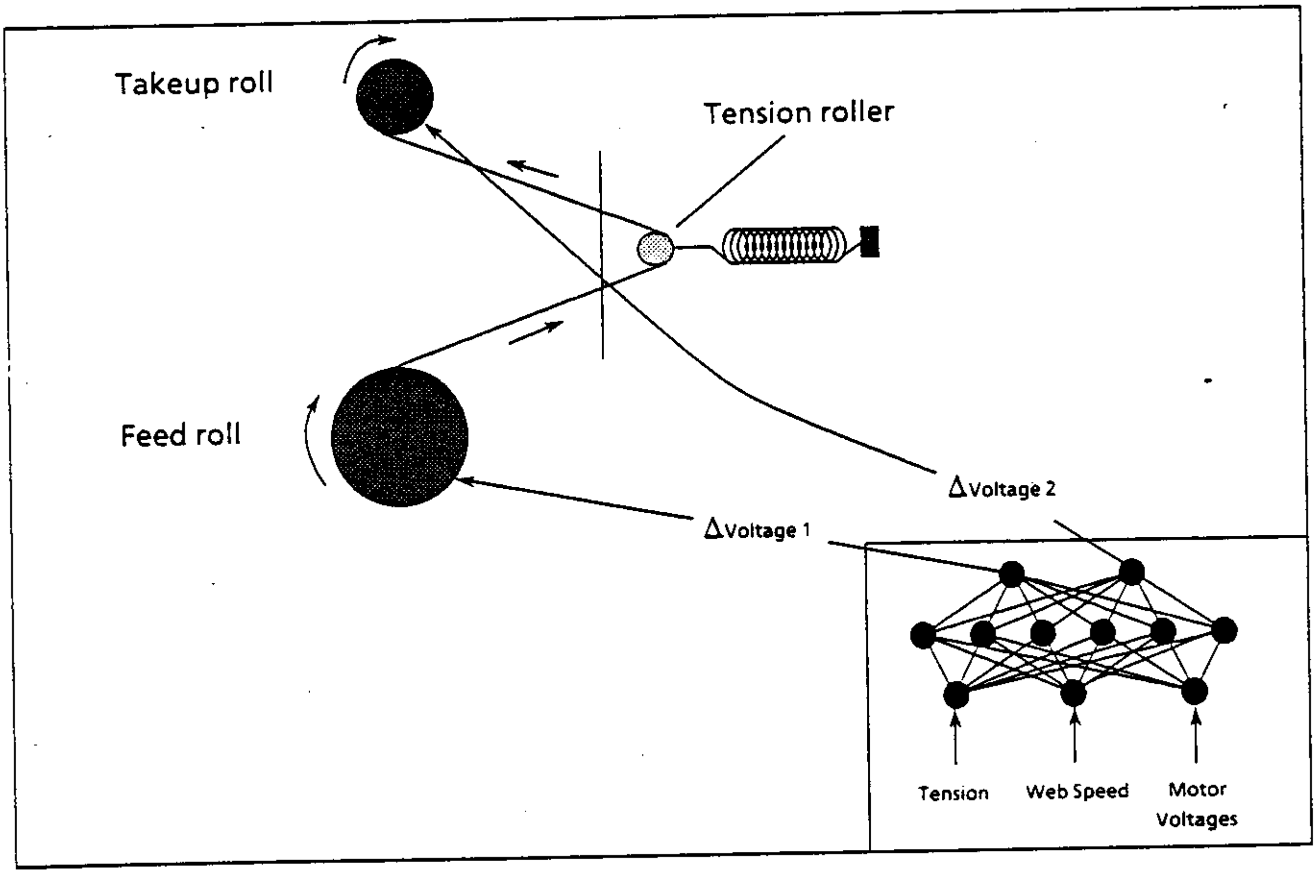

Web Winding controlled by AI-NET

Fig 23

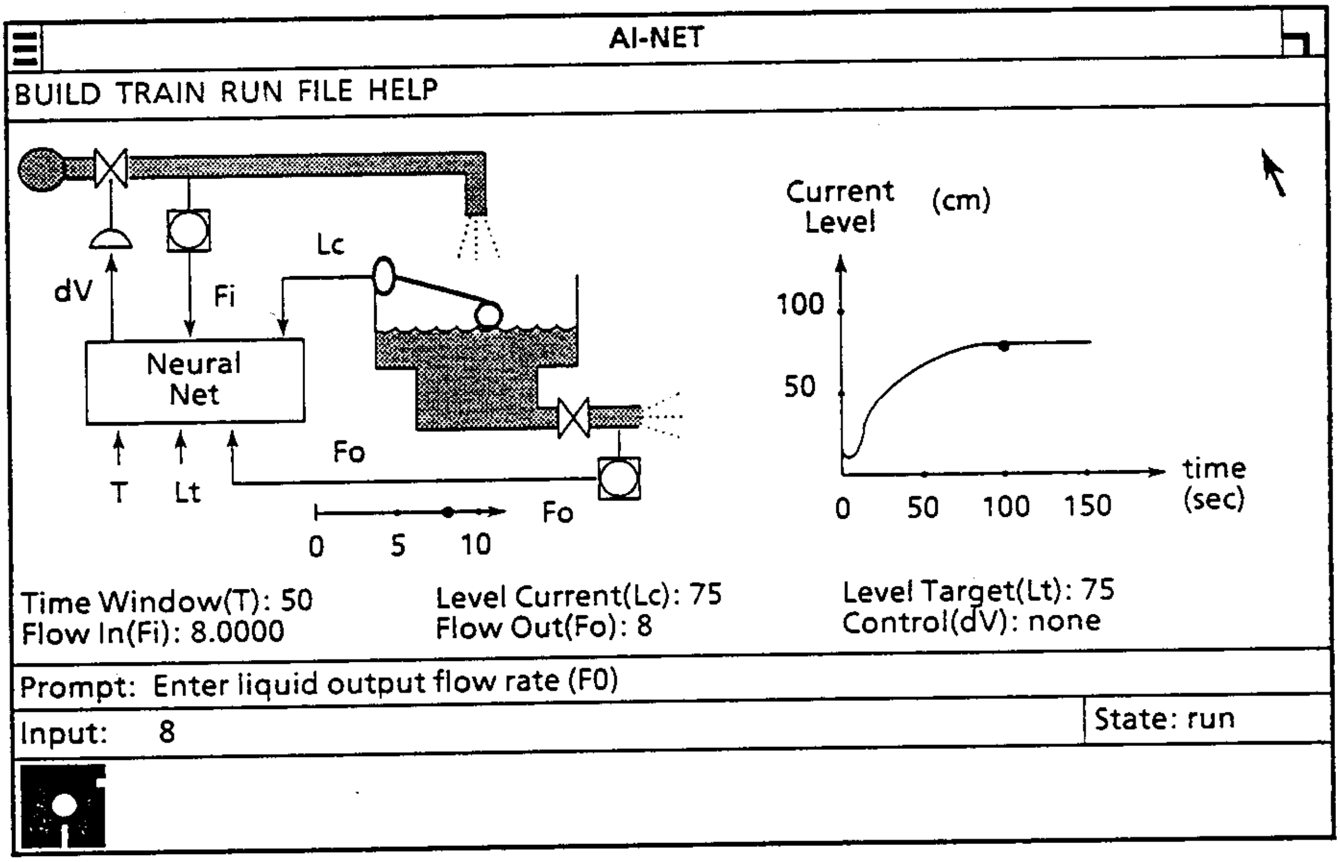

Time Window(T): 50
Flow In(Fi): 8.0000

Level Current(Lc): 75
Flow Out(Fo): 8

Level Target(Lt): 75
Control(dV): none

Prompt: Enter liquid output flow rate (F0)

Input: 8

State: run

Tank Filling Controlled by AI-NET

Fig 14

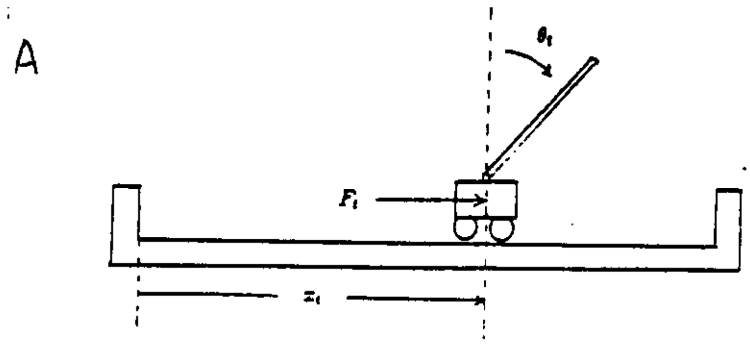

The Pole-Balancing Environment

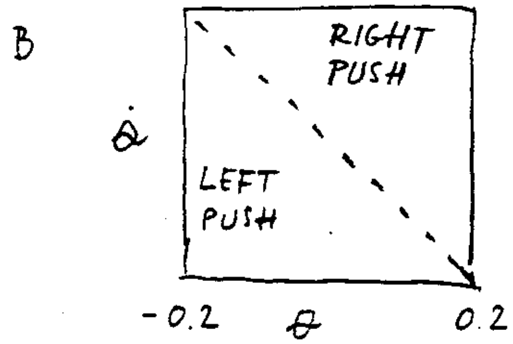

FIG. 25

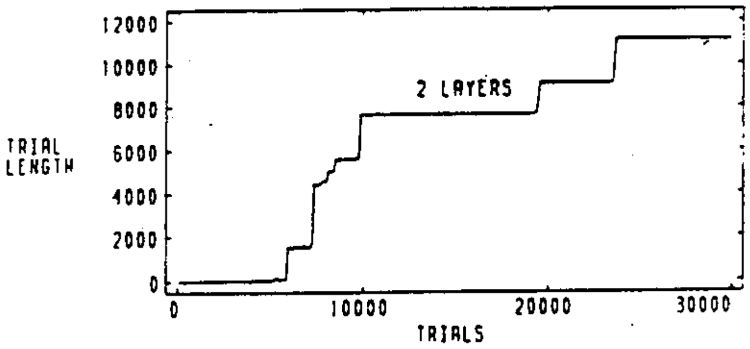

Figure 26 Balancing Time versus Trials for Two-Layer System

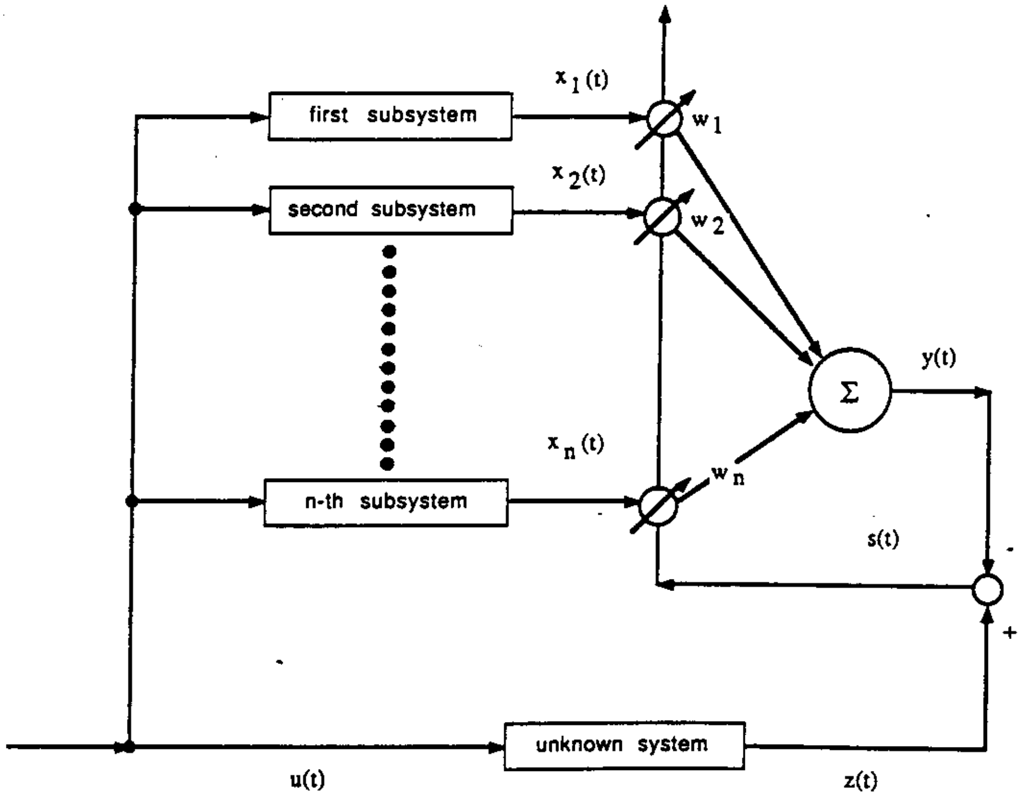

FIG 22 . A neural identifier of an unknown nonlinear system comprises many nonlinear subsystems and a neuron with heterosynaptic plasticity.

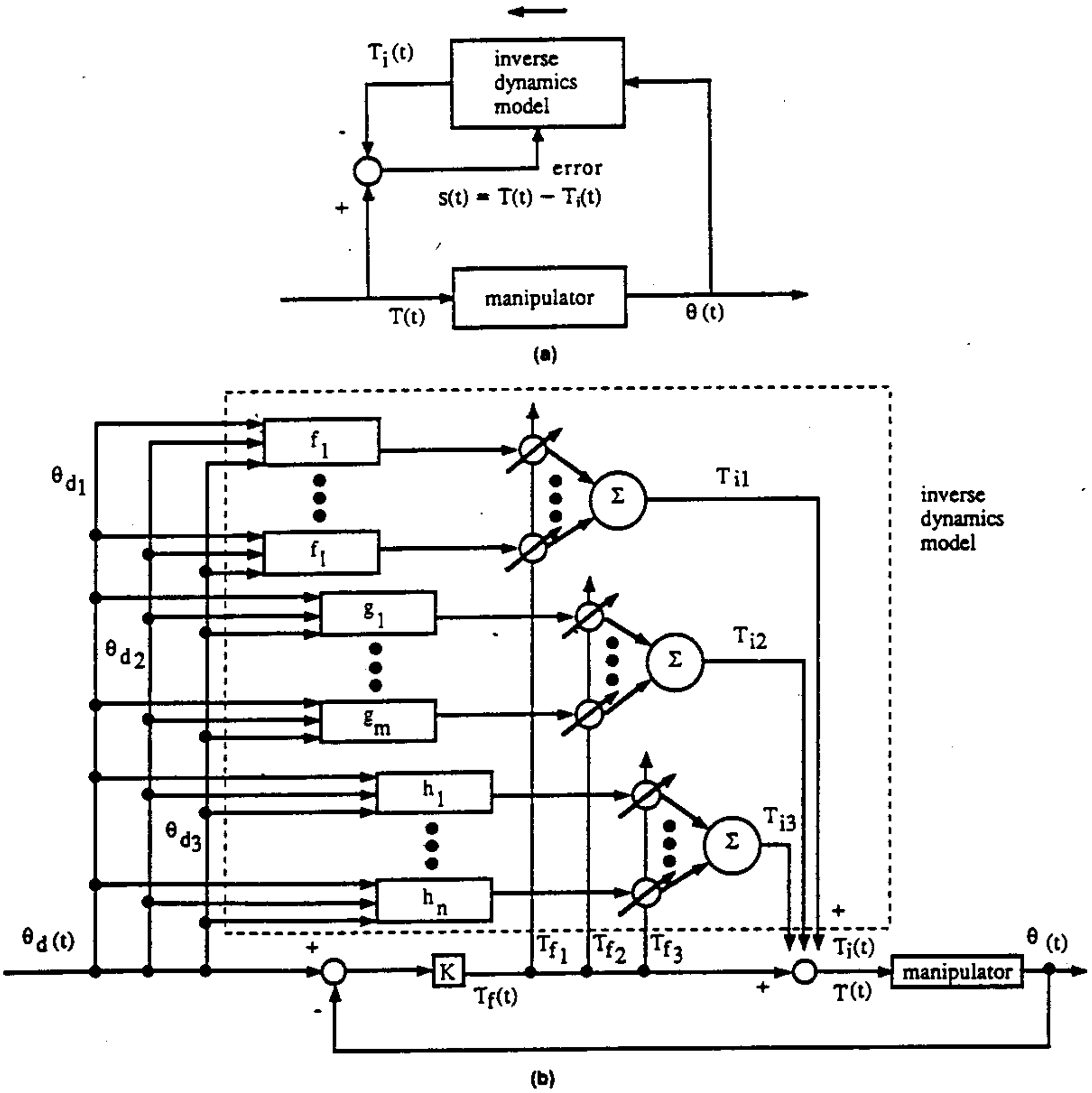

FIG. 2.9 Learning schemes of the inverse-dynamics model of the controlled system. (a) The simplest learning method. The arrow shows the direction of signal flow in the inverse-dynamics model. (b) The feedback-error-learning scheme and internal structure of the inverse-dynamics model for a three degree of freedom robotic manipulator.